THE BALTIC JOURNAL
OF ROAD
AND BRIDGE
ENGINEERING
2024/19(4)

ISSN 1822-427X/eISSN 1822-4288
2024 Volume 19 Issue 4: 96–118
https://doi.org/10.7250/bjrbe.2024-19.650

DETERMINATION OF DEGRADATION AND COMPRESSIVE STRENGTH OF POLYURETHANE RESIN APPLIED FOR BRIDGE ABUTMENT

ŠARŪNAS SKUODIS[1], NERINGA DIRGĖLIENĖ[2*], MINDAUGAS ZAKARKA[3], DOVILĖ VASILIAUSKIENĖ[4]

[1–3]*Department of Reinforced Concrete Structures and Geotechnics, Vilnius Gediminas Technical University, Saulėtekio al.11, LT-10223, Vilnius, Lithuania*
[4]*Department of Chemistry and Bioengineering, Vilnius Gediminas Technical University, Saulėtekio al.11, LT-10223, Vilnius, Lithuania*

Received 8 July 2024; accepted 13 November 2024

Abstract. This study is carried out in order to review the deformation properties, strength, applications and suitability of polyurethane resin as a ground improvement method applied for bridge abutment construction. Since it is applied in the ground, awareness on polyurethane degradation needs to be emphasised. Deformation properties were determined for resin injections before and after degradation. The degradation of samples was studied by exposure to gasoline, diesel, oil, NaCl salt solutions with different concentrations (59, 193 and 301 kg/m^3) and a mixture of fungi. After the degradation tests, compressibility tests were also performed. The use of resin as a ground improvement method has several advantages over conventional methods. The

* Corresponding author. E-mail: neringa.dirgeliene@vilniustech.lt

Šarūnas SKUODIS (ORCID ID 0000-0001-9467-7255)
Neringa DIRGĖLIENĖ (ORCID ID 0000-0002-3628-9286)
Mindaugas ZAKARKA (ORCID ID 0000-0001-7154-1267)
Dovilė VASILIAUSKIENĖ (ORCID ID 0000-0001-8837-6499)

information presented enables road and bridges engineers and construction professionals to make competent decisions about implementing this innovative technique in the projects.

Keywords: bridge abutment, compressive strength, degradation, ground improvement, polyurethane resin, road embankment.

Introduction

Roads, bridges and structures are affected by many factors, which can cause serious damage. Problems such as subsidence, collapse can happen due to factors like material loss, poor construction, structural sinking, heavy traffic, and climate changes. Traditional repair methods such as asphalt overlay, cement grout and crack sealing only provide temporary solutions by fixing surface issues without addressing the reason. These methods can also make things worse by adding extra weight to already stressed soil leading to frequent repairs. Full-depth reconstruction is an option, but it is time-consuming, requires long road closures and is expensive. Therefore, there is a need for quick, practical solutions that keep roads in long exploitation, reduce the need for frequent repairs and shorten repair times. Any road and soil repairs should provide adequate strength and uniform surface level to ensure vehicle safety on expressways (Bian et al., 2021).

The polyurethane foams have been widely applied in multiple industries such as building construction, automotive industry, airport runways, ballasted railways and refrigerator over the recent years because of great mechanical properties, high weight-carrying capacity, low apparent density, excellent thermal insulating properties and good resistance to various weather conditions (Blake, 2022; Buzzi et al., 2010; Lat et al., 2020; Somarathna et al., 2018; Yang et al., 2019). Permeable polyurethane improves an embankment compaction degree and mechanical properties (Wang et al., 2021). A structural polyurethane foam injected into voids beneath concrete slabs, walkways, foundations, walls, stabilises the underground and lifts it to the desired height without excavation (Guo et al., 2020; Saleh et al., 2019). The injection process is simple and efficient requiring less equipment and labor compared to other techniques used in the field, and it has no adverse effects on soil ecology or groundwater levels (Sabri et al., 2021). To obtain stress-strain curves, mechanical experiments must be conducted (Wei et al., 2017). The deformation modulus of the soil is a crucial parameter for assessing soil stiffness and designing constructions. This modulus varies based on numerous factors, including soil type, depth, moisture content, applied load, and other conditions (Tamošiūnas et al., 2022).

Polyurethane polymer grouting material under uniaxial pressure should go through three stages: elasticity, yielding and densification. At the elastic stage, the strain develops relatively quickly. The stress at the yield plateau stage is used as a representation of the compressive strength. As density increases, material strength increases rapidly, at the density stage, the dense specimen gradually shows brittle failure (Xiang et al., 2017).

For low-density polyurethane foam (LPF), the stress-strain behavior delineates three distinct stages as described above. During the linear elastic stage and towards the end of the densification stage, the stress of LPF noticeably increases with strain. Within the plateau region, stress augmentation occurs more slowly as strain rises, demonstrating elastoplastic properties in LPF mechanical characteristics. Cell structure failure occures during the plastic stage, marking it as LPF failure stage (Liu et al., 2019).

However, high-density polyurethane foam (HPF) exhibits an atypical brittle characteristic after the linear elastic stage as the compressive stress does not sharply decline after failure. Hence, the stress-strain curves should be distributed into four stages: linear elastic stage, brittle stage, plastic stage, and densification stage. Cell structure failure in HPF initially transpires during the brittle stage and subsequently in the plastic stage, making both stages the failure points for HPF (Liu et al., 2019).

From uniaxial compression experimental tests, the stress-strain curve depicting the mechanical characteristics of rigid polyurethane foams across various strain rates and temperatures was derived. Quantitative analysis of the influence of strain rate and temperature on mechanical behavior and energy absorption was conducted based on these experimental findings. Results revealed that at low temperatures and high strain rates, rigid polyurethane exhibited significantly enhanced mechanical properties including yield stress, plateau stress and energy absorption. However, neither temperature nor strain rate affected the optimal energy absorption state of this polymer (Zhang et al., 2022).

The analysis of the plate load test results demonstrated a significant impact of the injected polyurethane resin on the properties of the soil. After the resin injection, the deformation modulus of the soil increased substantially. The resin also had a noticeable effect on the density of the sandy soil (Sabri & Shashkin, 2018).

Low exothermic polyurethane grouting material is utilised for road reinforcement and repair in frozen earth regions. The findings indicate that temperature significantly affects the material properties (Constantinescu & Apostol, 2020; Shi et al., 2010). As temperature

decreases, the material expansion properties decrease too, while its tensile and compressive properties increase. However, lower temperatures also make the material more brittle, as observed in the failure mode. The low exothermic polyurethane grouting material effectively minimises vertical deformation caused by wheel loads in damaged areas. This study serves as a reference for road reinforcement and repair projects in cold climates (Zhong et al., 2023).

Soil injection using polyurethane resin is effective but has limitations. One challenge is achieving uniform resin distribution due to soil variations in permeability and heterogeneity, leading to uneven consolidation (Hao et al., 2018). It is also less effective in highly compacted or heavily cemented soils where penetration is difficult. Another issue is estimating the correct injection volume and pressure. Too little volume can result in incomplete consolidation, while too much can cause resin wastage and excessive uplift pressure. Monitoring and control of the injection process are essential. Numerous studies using lab tests, field measurements, and numerical modelling have evaluated the effectiveness of the technique, focusing on load-bearing capacity, settlement reduction and long-term stability (Dirgėlienė & Kordušas, 2023).

By employing the volumetric foam hardening material model, it was illustrated that the simulated force-time history data closely aligned with experimental results of polyurethane foam across quasi-static to dynamic (600–2.600 s^{-1}) strain rates. This validation enables using the foam material model in exploring numerous dynamic foam material tests in future research (Whisler & Kim, 2015).

To optimize the application of soil injection with polyurethane resin, ongoing research is focusing on severl aspects. These include optimal grouting volume, pressure and spacing (Guo et al., 2019). Moreover, these findings are important in assessing lifting efficiency and durability, thereby leading to the sustainability of railway track systems (Huang et al., 2024).

The results have generally been positive with the resin improving the mechanical properties of the treated soil. The injection process can enhance the soil shear strength, stiffness, and bearing capacity. However, the effectiveness of the technique may vary depending on site-specific conditions, such as soil type, depth, and environmental factors (Sabri et al., 2018).

The researchers determined that the results obtained from sea aging after five years of immersion indicated that polyurethane resin retain 100% of their initial tensile properties (Peter & Guy, 2007). The fungal attack studies revealed that polyester was more susceptible to fungal and bacterial attack than polyether while polyether was moderately

resistant to fungi and bacteria. In applications where a polyether is in regular contact with soil in either hot or humid environments, this material is able to resist microbial attack. Thus, polyether is often used in the cable industry (Howard, 2012).

When structural expanding polyurethane foam is inserted into the soil, it will be affected not only by the mechanical factors of the soil, but also by chemical and biological ones in the environment. The soil of the road structure will most likely be exposed to organic chemicals: fuel (gasoline, diesel) or automotive oils, and inorganic chemicals to sodium chloride NaCl salt and its solutions of various concentrations. Biological factors are microorganisms in the environment and their communities, consisting of fungi, bacteria, and protozoa. Fungi are usually the first colonizers of microbial communities in the natural environment. When testing the resistance of various construction, thermal insulation materials and coatings to microorganisms, fungi are selected in accordance with Lithuanian standart LST EN ISO15457:2022. At the time when fungi break down natural (cellulose, starch, etc.) polymers, their growth is visible after three days, when synthetic ones, which are produced from polymeric materials, are obtained from petroleum (polyester, polyethylene, acrylic coatings, etc.) under favourable growth conditions can be observed after seven days, according to the decrease in molecular weight of materials (Zeghal et al., 2021).). Fungal activity, including the growth of aerial mycelium on various surfaces, can be observed macroscopically without the aid of stereoscopic or microscopic equipment within 7–28 days, when the ambient humidity is not lower than 55±5% and the temperature is 24±2 °C. Particularly favourable conditions for the growth of fungi are humidity 70±5% and temperature 21±2 °C. Micromycetes easily adapt to various nutrient sources in the presence of excess moisture, they produce many enzymes capable of breaking down various substances of natural or synthetic

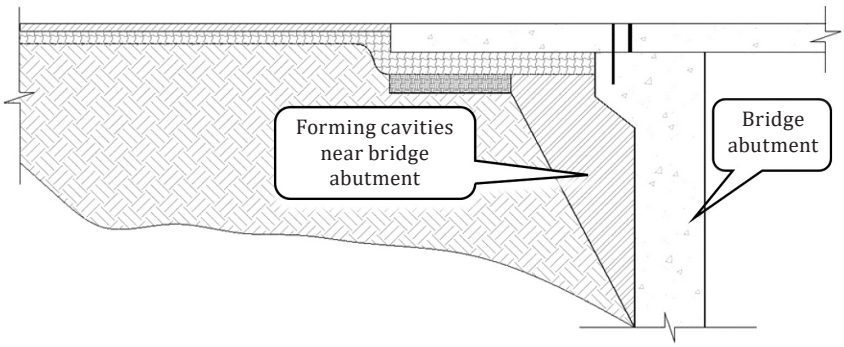

Figure 1. Forming cavities near bridge abutment

origin. Such materials lose their durability, mechanical, and aesthetic properties.

As the polyurethane-grouted subgrade has good dynamic stability under long-term train loads (Bian et al., 2021) it can be used to fill cavities near bridge abutment (Figure 1). Further investigation and development of the polyurethane resin are needed to improve the technique and create detailed design guidelines for different soil and environmental conditions.

The aims of this study are to evaluate the loads caused by road transport in the soil embankments close to bridge abutments and to determine the deformability properties before and after the degradation tests of polyurethane resin injections.

1. Evaluation of road construction loads

In Lithuania, the road construction loads can be selected according to different standards and regulations: KPT SDK 19 Rules for the design of standardized road surface structures for automobiles and KTR 1.01:2008 Road Technical Regulation "Automobile Roads". KPT SDK 19 provides two methods for determining the design load. The first one is used when the average intensity of heavy traffic per day is known. The second is considered a priority when determining the design load for highways and country roads. This method requires vehicle axle loads. Axle loads are determined based on data from traffic weighting (dynamic weighting) or weighting posts (static weighting). Also, axle

Table 1. The loads on the road structure according to KPT SDK 19

Vehicle class		4-axle truck	Load on the support, kPa	2-axle bus	Load on the support, kPa	3-axle truck with 3-axle trailer	Load on the support, kPa
Average fully loaded vehicle weight, t		27.3		16.6		36.2	
Weight distribution, %	1 axle	20.7	394.7	34.7	402.4	17.7	444.7
	2 axle	20.6	392.8	65.3	757.2	20.3	510.0
	3 axle	30.7	585.4	-	-	18.3	459.8
	4 axle	28.0	533.9	-	-	15.9	399.5
	5 axle	-	-	-	-	13.9	349.2
	6 axle	-	-	-	-	13.9	349.2

Note: Loads are distributed in a circle with a diameter of 0.3 m (16 vehicle classes in total).

Table 2. The loads on the road structure according to KTR 1.01:2008

Concentrated load, kN	Load on the support, kPa
115.0	813.9
100.0	707.5

Note: Loads are distributed in a circle with a diameter of 0.3 m.

loads can be determined based on vehicle classes and theoretical axle weight distribution. These data are presented as sixteen vehicles of different weight, which have a different number of axles and different weight distribution to the axles (Table 1). KPT SDK 19 does not define the distance between the axles, so when evaluating the vertical loads generated in the road structure and their propagation in the road structure, the most unfavorable distance specified by LST EN 1991-2 is accepted. The axle load is assumed to be distributed over the surface of a circle with a diameter of 0.3 m.

KTR 1.01:2008 provides very incomplete permissible axle loads. The size of the design load on the axle of the car depends on the type of road. During the construction and reconstruction of main and country roads, the load on the car axle is 115 kN, during the construction and reconstruction of other roads – 100 kN (Table 2). Due to the lack of a more detailed definition of loads, assumptions have to be made. They are adopted the same as in the case of KPT SDK 19 – the distance between the axes is equal to 0.5 m, and the area to which the load is distributed is a circle with a diameter of 0.3 m.

One of the tasks of this research is to assess the loads imposed by road vehicles on soil embankments and calculate the resulting vertical stresses. Using the calculated vertical stresses, it is possible to determine the depth of stress distribution while based on horizontal stresses, an appropriate lateral pressure (representing embankment loads) can be selected for tests conducted with a triaxial compression apparatus.

The loads from vehicles in the embankment induce additional vertical and horizontal stresses. Based on the calculated vertical stresses, it is possible to determine the depth of stress distribution. The calculations were performed using the Boussinesq solution. The highest values of vertical stress occur along the load application axis. Increasing depth, results decrease in stress, as well as moving away from the load application axis leads to a reduction in stress. The stress is considered negligible when it becomes equal to or less than 10% of the initial value. The results of stress distribution calculations are presented in Figure 2.

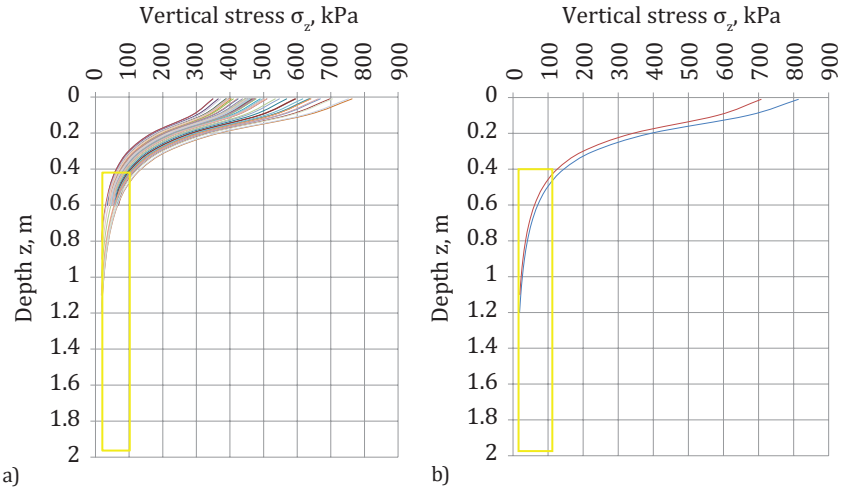

Figure 2. Distribution of vertical stresses (the yellow zone marks the structure of the soil base, which is subjected to vertical stresses according to Table 3: a) according to KPT SDK 19; b) according to KTR 1.01:2008)

The calculated results of vertical stress σ_z propagation according to KPT SDK 19 and KTR 1.01:2008 are presented in Table 3. The highest values are determined at the embankment surface. The maximum vertical stress of 813.62 kPa was formed during calculations according to KTR 1.01:2008. The vertical stress varies from 813.62 to 707.5 kPa at the embankment surface. When calculating according to KPT SDK 19, the

Table 3. Maximum values of vertical stresses occurring in the road structure

Part of the road embankment structure	Depth, m	Vertical stresses in the road structure, kPa	
		KPT SDK 19	KTR 1.01:2008
Road surface construction	0.01	752.33	813.62
	0.10	619.18	669.61
	0.20	363.06	392.61
	0.30	212.17	229.45
Construction of soil embankment	0.40	133.93	144.84
	0.50	90.82	98.22
	0.60	65.18	70.49
	0.70	48.87	52.85
	0.80	37.92	41.01

vertical stress is 8% lower, i.e., 752.33 kPa, and it varies till 349.23 kPa. For both vertical stresses, 10% of the initial vertical stress value was determined at a depth of 0.56 m. The area over which the load is distributed has the greatest influence on the depth of stress propagation. The smaller the area, the shallower the stress propagation depth.

Proper assessment of road loads and stress propagation in the road structure allows selecting test loads in the laboratory and comparing the obtained results with the magnitudes of the propagated stresses.

2. Degradation study of polyurethane foam

2.1. Material and sample preparation

Polyurethane foam is a polyol formulation, which, mixed in the appropriate ratio with georesin hardener, generates an expandable foam with a free rise density between 40 and 60 kg/m^3. The foam hardens within a few minutes. The tested polymer resin samples were prepared by injection mixtures, which must achieve a density of 50 kg/m^3. The samples of polyurethane were made for injections without lateral restraint, i.e., representing the filling of large voids with free flow of polymer. Such situations can arise in the filling of bridge abutment cavities. It should be noted that when studying specimens prepared with free flow, the most unfavoruable properties of polymers are determined, i.e., if polyurethane foam is injected with lateral restraint, their properties are usually 1.5–4 times better than without lateral restraint. It appeared that the samples had been produced from larger blocks formed with free flow injection and after hardening by cutting in the form of cylinder with a diameter of 86 mm, a height of 34 mm and the density ranging from 41.43 to 77.23 kg/m^3. The deformation properties of polymers resin were determined with a uniaxial compression apparatus applying rings (constraining horizontal deformations).

2.2. Evaluation of polymer degradation

The fungi were used for microbiological degradation studies of geopolymer according to Lithuanian standart LST EN 16492:2014 for the use of fungi in the field conditions: DSM3042 *Aureobasidium pullulans*; DSM 12633 *Alternaria alternata*; DSM19653 *Cladosporium cladosporoides* and DSM 6308 *Ulocladium atrum*. The fungi were first grown on saturated nutrient microbial PDA (potato dextrose agar) medium until sporulation for 7–21 days at 23 °C, 55% humidity. The fungi spores were collected with 0.9% NaCl solution and diluted to 10^6 spores/ml. These

microorganism spore suspensions were mixed in equal parts and 5 ml each were applied to the polymer samples. The chemical degradation of polymer was carried out with gasoline (E10), diesel fuel, motor oil and NaCl solutions. The concentrations of NaCl solutions (59 kg/m^3, 193 kg/m^3, 301 kg/m^3) were chosen based on the textbook (Čygas et al., 2016), applying 5 ml each on the prepared expandable foam samples. For degradation tests, 5 samples were exposed to gasoline (E10), 3 samples exposed to diesel, 3 exposed to motor oil, 1 exposed to NaCl (59 kg/m^3) salt, 1 exposed to NaCl (193 kg/m^3) salt, 1 exposed to NaCl (301 kg/m^3) salt, and 3 samples affected by fungi mixture.

Table 4. The results of geopolymers incubated with chemical and microbiological agents in an aerobic environment

Degradation agents	Samples with degradation agent	Samples with the product after 35 days of degradation (incubation conditions: 75% humidity at 23 °C)	Stereoscopic analysis after 35 days of incubation
Gasoline (Samples No. 3; 15)			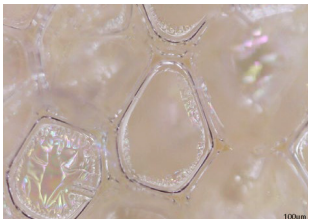 Magnification 400×.
Diesel (Sample No. 14)			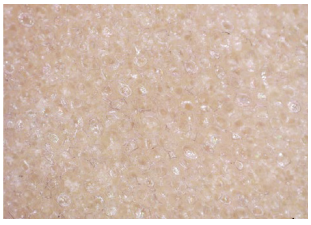 Magnification 40×.
Oil (Sample No. 8)			 Magnification 40×.

Degradation agents	Samples with degradation agent	Samples with the product after 35 days of degradation (incubation conditions: 75% humidity at 23 °C)	Stereoscopic analysis after 35 days of incubation
Fungi mixture: *A. pullulans; A. alternata; Cl. Cladosporoides; U. atrum* (Sample No. 6)	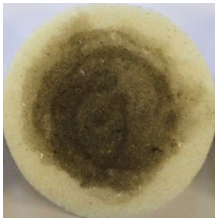		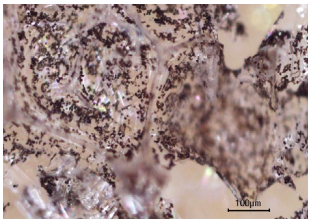 Magnification 400×.
NaCl (59 kg/m^3) (Sample No. 10)			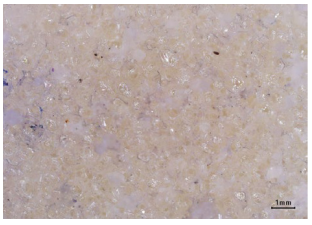 Magnification 40×.
NaCl (193 kg/m^3) (Sample No. 11)			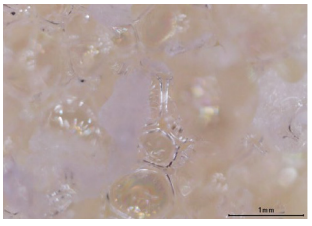 Magnification 75×.
NaCl (301 kg/m^3) (Sample No. 12)			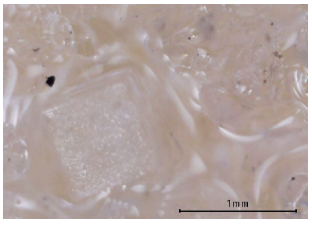 Magnification 100×.

All expandable foam samples for chemical and microbiological degradation tests were incubated for 35 days at 23 °C, 75% humidity taking pictures every 7 days and visually evaluating them (Table 4). If fungi can disrupt prepared samples, then growing of the aerial

mycelium is visible after 7–21 days, so the period of 35 days is sufficient to determine these mixed microorganisms (*A. pullulans; A. alternata: C. Cladosporoides, U. atrum*) activities on the surface of expandable foams. Analysing the samples coated with gasoline, diesel, and oil, it can be seen that the surface of the polymer membranes has a beautiful solid structure. In some places the damage caused by cutting the sample can be seen, the sample with oil pores are filled with oil (Table 4). Examining the samples inoculated with fungi mixture, it can be observed that the surface of the polymer membranes is abundantly covered with spores of microorganisms, but there is no indication of their growing as aerial hyphae or biofilm is not visible. It is believed that the tested polymer cannot be a source of nutrients for *fungi A. pullulans, A. alternata: Cl. Cladosporoides, U. atrum*. The surface of the polyurethane was intermittently covered with NaCl crystals. The geopolymer membrane surfaces exhibited varying degrees of NaCl crystal coverage (Table 4). Samples exposed to the 59 kg/m^3 NaCl concentration displayed incomplete coverage, but samples exposed to the 193 kg/m^3 NaCl solution exhibited more complete coverage with visible NaCl crystals ranging from 0.5 to 1 mm in size than 59 kg/m^3. Samples treated with the highest concentration (301 kg/m^3 NaCl) showed abundant layer of NaCl crystals (0.5–1 mm) completely covering the surface. Some membrane surfaces displayed the damage consistent with sample cutting procedures, as observed in Specimen No. 8 (Table 4). Notably, typical cutting-induced pores were obscured by the NaCl solution. This solution absorbs water vapor at the test conditions (75% humidity, 23 °C), suggesting the polymer surface was directly immersed in the NaCl salt solution.

2.3. Evaluation of compressibility of polyurethane foam

The compressive strength and elasticity modulus of polymers can be determined using an oedometric device. Since there is no approved standard for these tests, test standards were selected that apply to soil tests as polyurethane injections were intended for soil strengthening. The maximum permissible deformation of the sample was selected according to Lithuanian standard LST EN ISO 17892-8:2018. Tests were performed by compressing the samples up to 15% deformation. The loading speed was selected according to Lithuanian standard LST EN ISO 17892-7:2018. All specimens were compressed at a strain rate of 0.05 mm/s. Results were processed according to LST EN ISO 17892-5:2017.

The compressibility properties were determined for polymer injections material that were not affected by anything (labelled “natural”

Table 5. The results of compressibility tests

Title	Sample No.	Density, kg/m^3	Maximum load, N	Area, cm^2	Maximum compressive stress, kPa	Elasticity modulus, MPa
Natural	1	57.06	1479.4	58.77	254.81	3.40
Natural	4	54.55	2390.6	58.77	406.78	5.95
Natural	5	53.60	2062.3	58.99	347.09	6.23
Natural	6	53.80	2133.9	58.77	367.54	7.27
Natural	7	53.51	1546.7	58.54	266.40	4.88
				Average	342.53	5.55
Gasoline	1	54.07	1433.1	56.30	252.68	5.35
Gasoline	2	47.76	1421.1	56.97	256.56	4.33
Gasoline	3	49.95	1491.2	57.41	259.74	5.36
Gasoline	15	47.31	1651.9	57.19	284.52	6.34
Gasoline	17	41.43	1026.9	57.41	181.06	2.89
				Average	251.87	4.85
Diesel	4	63.27	2027.3	57.41	357.45	7.52
Diesel	5	64.79	1727.0	56.97	304.50	5.20
Diesel	14	56.96	1516.6	57.19	261.22	4.55
				Average	307.72	5.76
Oil	7	72.56	1673.7	56.75	295.10	4.47
Oil	8	77.23	1521.5	56.75	268.27	3.82
Oil	9	74.12	1767.7	56.75	311.67	4.69
				Average	291.68	4.33
NaCl (59 kg/m^3)	10	50.08	1653.3	58.09	284.76	4.51
NaCl (193 kg/m^3)	11	52.69	1579.7	58.09	272.09	3.21
NaCl (301 kg/m^3)	12	55.30	1816.8	58.09	312.93	4.13
				Average	223.26	3.95
Fungi mixture	6	51.60	1585.3	56.97	279.51	4.37
Fungi mixture	13	47.42	1387.5	57.19	244.64	3.88
Fungi mixture	16	45.83	1038.8	57.19	178.92	2.75
				Average	234.36	3.67

in Table 5), 5 samples were prepared for this purpose. Also, 17 samples affected by chemical and microbiological material were compressed: 5 samples exposed to gasoline, 3 samples exposed to diesel, 3 exposed to oil, 1 exposed to NaCl (59 kg/m^3) salt, 1 exposed to NaCl (193 kg/m^3) salt, 1 exposed to NaCl (301 kg/m^3) salt, 3 samples affected by fungi mixture.

After the degradation tests, the compressibility tests were performed on the specimens. Only the results of successful tests are presented. Other samples were rejected due to poor cutting quality. The initial data and results of the compressibility of the specimens are presented in Table 5.

Detailed compression graphs of polymer samples (unaffected and affected by degradation agents) are presented in Figures 3–8. The compressive stress and deformation responses can be divided into three different parts. In the first part, generally up to 15% of strain, material demonstrated linear elastic deformation because of elastic bending and stretching of material cells. The second part (plateau) began when sample experienced failure due to plastic bending. When mostly polyruathane cells experienced plastical failure, the cells walls started to interact with each other and led to a fast increase in the stress. This part is called the densification. The samples in Figures 3–8 did not achieve the third part. Elasticity modulus is defined as the ratio of the linear stress and to its corresponding strain. Compressive strength, which can also be as yield stress or peak stress σ_y, is the stress at the yield point if a yield point occurs before 15% strain or, in the non-existance of such a yield point, the stress is at 15% strain (Rahimidehgolan & Altenhof, 2023). It can be seen in this study that some samples reached peak stress before 15% strain, and

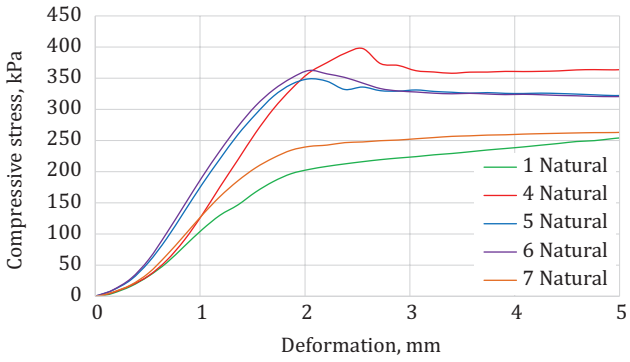

Figure 3. The relation of the compressive stress and deformations of unaffected samples

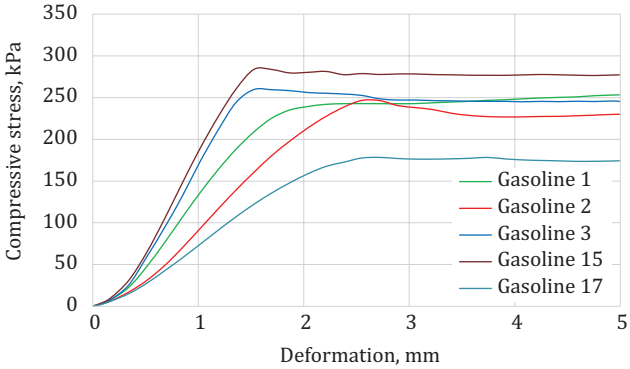

Figure 4. The relation of the compressive stress and deformations of samples exposed to gasoline

compressive strength of some samples was determined at 15% strain. The densification strain is the critical strain, at which the cell walls and edges begin to interact with each other. The densification strain is the point, at which the cellular structure becomes fully compacted. Then the material starts to behave like its base solid material than cellular.

The determined maximum compressive strength of the investigated polymers resin specimens ranges from 178.92 to 406.78 kPa (Table 5). The lowest value of the compressive strength was obtained for the sample coated with fungi mixture, whose density was 45.83 kg/m^3. The highest value was determined for natural specimen with density of 54.55 kg/m^3. The density of natural specimens varies from 53.51 to 57.06 kg/m^3 and compressive strength varies widely from 254.81 to

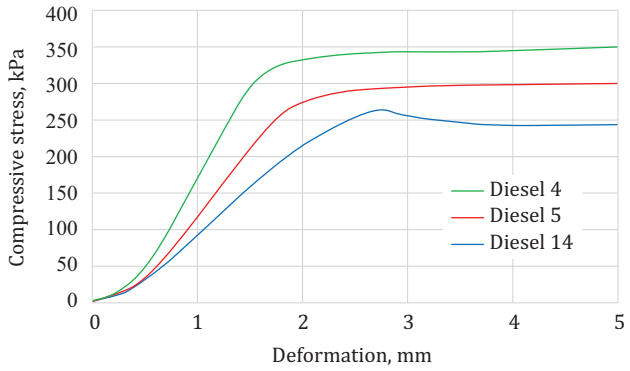

Figure 5. The relation of the compressive stress and deformations of samples exposed to diesel

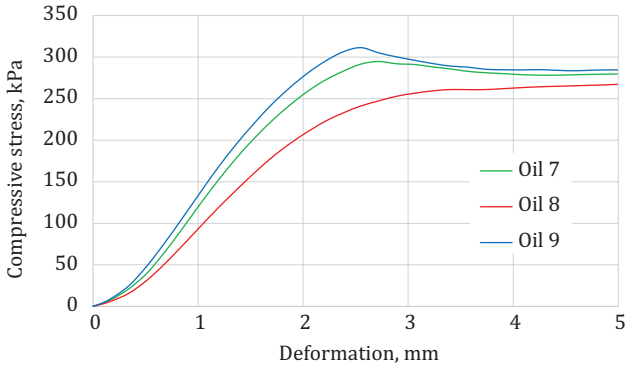

Figure 6. The relation of the compressive stress and deformations of samples exposed to oil

476.78 kPa. It is obvious that the size of the compressive strength does not depend on sample density, which ranges from 45.83 kg/m^3 to 77.23 kg/m^3 for all specimens. The compressive strength can be reduced by heterogeneity of samples stucture (Buzzi et al., 2008). Literature analysis shows that the yield stresses in both rising and transverse directions are very similar and limited to values between 250 and 500 kPa (Buzzi et al., 2008). Specimens, formed in the laboratory and incorporating contact planes, display a lower compressive strength compared to homogeneous material. The homogeneity of the sample can be ensured in the laboratory, but the heterogeneity of the sample is obtained when injecting into the soil.

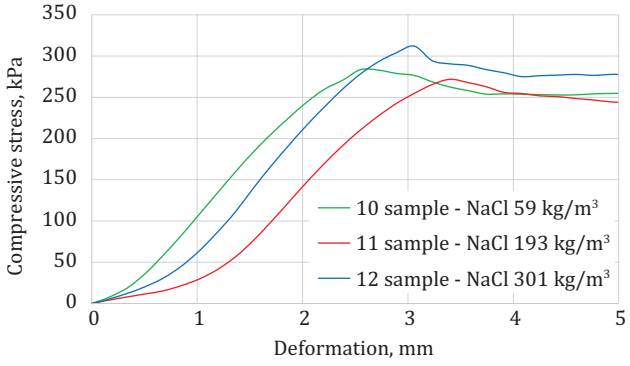

Figure 7. The relation of the compressive stress and deformations of samples covered by NaCl

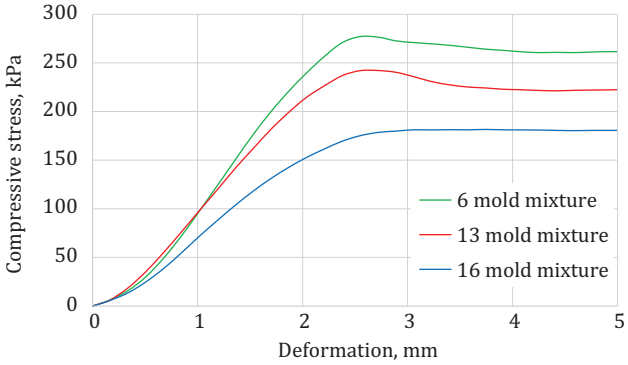

Figure 8. The relation of the compressive stress and deformations of samples affected by fungi mixtures

The elastic state of the specimens ends when the deformations reach a value of 1.5–2.6 mm (4–8% of strain). The largest deformations of 2.0–2.6 mm (6–8% of strain) were achieved for samples coated with NaCl salt. It is not clear whether this is a trend or a coincidence, but a larger number of samples should be tested. The elastic modulus changes from 2.75 MPa to 7.52 MPa for all types of the samples. The smallest one was determined for the sample covered with fungi mixture and the biggest for the sample coated with diesel.

Table 5. The shape of the specimens before and after the test

Name	Sample No.	Sample view	
		Before cut	After cut
Natural	5		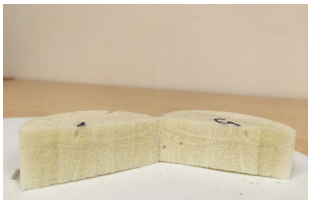
Gasoline	1		

Name	Sample No.	Sample view	
		Before cut	After cut
Diesel	4		
Oil	9	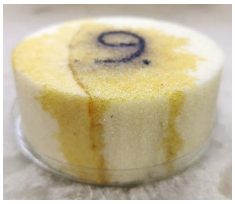	
NaCl (301 kg/m^3)	12		
Fungi mixture	6		

All specimens were cut in half after the degradation and compression tests to ensure that they were not penetrated and damaged by the chemical and microbiological agents. It should be noted that all the structural changes that were determined after cutting the samples were due to the unconstrained injection of the sample (injection technology). No structural changes were detected due to the compression test. Also, no structural changes were detected due to the degradation tests (Table 5).

The compressive stress and deformation relation allow estimating maximum acceptable stress and the deformation that is achieved. The maximum acceptable stress is determined as the stress that deviates from the linear behaviour in load-deformation relation.

3. Conclusions of polymer degradation and deformation research results

After carrying out tests with a uniaxial compression apparatus while restraining horizontal deformations, the strength and deformability properties of polymer samples were determined according to the selected representative loads of the road embankment structure. The calculated maximum compressive strength of the studied polymers ranges from 178.92 to 406.78 kPa. The determined compressive strength according to experiments is greater than the calculated vertical stress acting on the soil embankment (Table 3), which according to different standards is 133.93 to 144.84 kPa at a depth of 0.4 m and at a depth of 0.8 m from 37.92 to 41.0 kPa. No structural changes due to the compression or degradation tests were detected. In some specimens, transverse cracks in the center of the specimen were formed due to the application of unrestrained specimen injection technology. This explains the variation in compressive strength, which is between 178.92 and 406.78 kPa. It should be remembered that when studying specimens prepared with free flow, the most unfavourable properties of polymers are determined, i.e., if polyurethane foam is injected with lateral restraint, their properties are usually 1.5–4 times better.

After carrying out degradation tests of polyurethane foam with chemical and microbiological agents it was determined that:

1. Fungi *A. pullulans. A. alternata. Cl. cladosporoides. U. atrum* did not grow on the surface of the polymer under environmental conditions (75% of humidity and 23 °C), because this polymer was not decomposed, so biological degradation did not occur;
2. When working with the samples under environmental conditions of 75% humidity and 23 °C, the solubility of the samples was not determined with gasoline, diesel fuel or grease, so degradation did not occur;
3. When samples were exposed to NaCl solutions of 59, 193, 301 kg/m^3, crystalline NaCl derivatives formed and accumulated on the polymer.

Concluding this research findings, it can be stated that investigated polymer material can be applied for fullfiling bridge abutment cavities. However, this interpretation applies only to expansion resin injections with low densities.

Acknowledgements

The equipment and infrastructure of the Civil Engineering Scientific Research Center of Vilnius Gediminas Technical University was used for the investigations. The authors sincerely thank JSC Geolift Baltic for sample preparation and allowing the publication of this research, and anonymous reviewers for their constructive comments and suggestions for improving the quality of this article.

Funding

This research has been supported by the Center of Excellence project "Civil Engineering Research Centre" (Grant No. S-A-UEI-23-5).

JSC Geolift Baltic prepared the samples according to the project "Development of Geopolymer Injections" (Grant No. 02-019-K-0004).

REFERENCES

Bian, X., Duan, X., Li, W., & Jiang, J. (2021). Track settlement restoration of ballastless high-speed railway using polyurethane grouting: Full-scale model testing. *Transportation Geotechnic, 26*, Article 100381. https://doi.org/10.1016/j.trgeo.2020.100381

Blake, D. H. (2022). *Performance of resin injection ground improvement in silty sand based on blast-induced liquefaction testing in Christchurch, New Zealand* [Master's Thesis, Brigham Young University]. https://scholarsarchive.byu.edu/etd/9458/

Buzzi, O., Fityus, S., Sasaki, Y., & Sloan, S. (2008). Structure and properties of expanding polyurethane foam in the context of foundation remediation in expansive soil. *Mechanics of Materials, 40*(12), 1012–1021. https://doi.org/10.1016/j.mechmat.2008.07.002

Buzzi, O., Fityus, S., & Sloan, S. W. (2010). Use of expanding polyurethane resin to remediate expansive soil foundations. *Canadian Geotechnical Journal, 47*(6), 623–634. https://doi.org/10.1139/T09-132

Constantinescu, D. M., & Apostol, D. A. (2020). Performance and efficiency of polyurethane foams under the influence of temperature and strain rate variation. *Journal of Materials Engineering and Performance, 29*(5), 3016–3029. https://doi.org/10.1007/s11665-020-04860-4

Čygas, D., Laurinavičius A., Vaitkus A., & Ratkevičius T. (2016). Kelių ir gatvių priežiūra žiemą: mokomoji knyga. [Maintenance of roads and streets in winter: an educational book]. https://doi.org/10.20334/1566-S

Dirgėlienė, N., Kordušas, V. (2023). Stabilization of soil using polyurethane resin injection technology. In J. A. O. Barros, G. Kaklauskas, E. K. Zavadskas (Eds.), *Modern building materials. Structures and techniques*. *MBMST 2023. Lecture Notes in Civil Engineering* (605–611), *392*, Springer, Cham.
https://doi.org/10.1007/978-3-031-44603-0_62

Fakhar, A. M. M., & Asmaniza. A. (2016). Road maintenance experience using polyurethane (PU) foam injection system and geocrete soil stabilization as ground rehabilitation. *IOP Conference Series: Materials Science and Engineering*, *136*, Article 012004.
https://doi.org/10.1088/1757-899X/136/1/012004

Guo, C., Sun, B., Hu, D., Wang, F., Shi, M., & Li, X. (2019). A field experimental study on the diffusion behavior of expanding polymer grouting material in soil. *Soil Mechanics and Foundation Engineering*, *56*(9), 171–177.
https://doi.org/10.1007/s11204-019-09586-7

Guo, C., Yang, J., Shi, M., Cai, B., Li, Z., & Guan, H. (2020). Improvement of construction equipment and technology of super-thin cut-off walls with polymer. *Advances in Science and Technology of Water Resources*, *40*(3), 68–71. https://doi.org/10.3880/j.issn.1006-7647.2020.03.011

Hao, M., Wang, F., Li, X., Zhang, B., & Zhong. Y. (2018). Numerical and experimental studies of diffusion law of grouting with expansible polymer. *Journal of Materials in Civil Engineering*, *30*(2).
https://doi.org/10.1061/(ASCE)MT.1943-5533.0002130

Howard, G. T. (2012). Polyurethane biodegradation. In S. N. Singh (Ed.), *Microbial degradation of xenobiotics* (pp. 371–394). Springer, Berlin, Heidelberg. https://doi.org/10.1007/978-3-642-23789-8_14

Huang, Z., Su, Q., Liu, T., Huang, J., Wang, X., & Kaewunruen, S. (2024). Full-scale experimental and field investigations into expansion mechanism of foamed polyurethane and its lifting behaviors for repair and maintenance of railway slab track systems. *Polymers, 16*(3), Article 404.
https://doi.org/10.3390/polym16030404

Lat, D. Ch., Ali, N., Jais, I. B. M., Yunusc, N. Z. M., Razali, & R., Talip. A. R. A. (2020). A review of polyurethane as a ground improvement method. *Malaysian Journal of Fundamental and Applied Sciences*, *16*(1), 70–74.
https://doi.org/10.11113/mjfas.v16n1.1235

Lithuanian Road Directorate. (2019). *KPT SDK 19 Automobilių kelių standartizuotų dangų konstrukcijų projektavimo taisyklės* [Rules for the design of standardized road surface structures for automobiles].

Lithuanian Standardization Department. (2022). *LST EN ISO15457: 2022 Dažai ir lakai. Laboratorinis metodas. skirtas dangos plėvelės konservantų apsaugančių nuo grybų. veiksmingumui patikrinti* [Paints and varnishes. Laboratory method for testing the efficacy of film preservatives in a coating against fungi].

Lithuanian Standardization Department. (2014). *LST EN ISO 16492: 2014 Dažai ir lakai. Paviršiaus blogėjimo dėl dangoje atsiradusių grybų ir dumblių įvertinimas* [Paints and varnishes. Assessment of surface deterioration due to fungi and algae in the coating].

Lithuanian Standardization Department. (2017). *LST EN ISO 17892-5:2017 Geotechnical investigations and tests. Laboratory soil tests. Part 5. Oedometer testing of step-loaded soil*.

Lithuanian Standardization Department. (2018). *LST EN ISO 17892-7:2018 Geotechnical investigations and tests. Laboratory soil tests. Part 7. Uniaxial compression test*.

Lithuanian Standardization Department. (2018). *LST EN ISO 17892-8:2018 Geotechnical investigations and tests. Laboratory soil tests. Part 8. Triaxial compression test of unconsolidated undrained soil*.

Lithuanian Standardization Department. (2012). *LST EN 1991-2 Eurocode 1. Effects on structures. 2 Part. Bridge traffic loads*.

Liu, K., Liang, W., Ren, F., Ren, J., Wang, F., & Ding, H. (2019). The study on compressive mechanical properties of rigid polyurethane grout materials with different densities. *Construction and Building Materials, 206*(4), 270–278. https://doi.org/10.1016/j.conbuildmat.2019.02.012

Ministry of the Environment of the Republic of Lithuania. (2008). *KTR 1.01:2008 Kelių techninis reglamentas "Automobilių keliai"* [Road Technical Regulation "Automobile Roads"].

Peter, D., & Guy, E. (2007). Accelerated ageing of polyurethanes for marine applications. *Polymer Degradation and Stability, 92*(8), 1455–1464. https://doi.org/10.1016/j.polymdegradstab.2007.05.016

Rahimidehgolan, F., & Altenhof, W. (2023). Compressive behaviour and deformation mechanisms of rigid polymeric foams: A review. *Composites Part B*: *Engineering, 253*, Article 110513. https://doi.org/10.1016/j.compositesb.2023.110513

Sabri, M. M., Bugrov, A., Panov, S., & Davidenko, V. (2018). Ground improvement using an expandable polyurethane resin. *MATEC Web of Conferences*, *245*, Article 01004. https://doi.org/10.1051/matecconf/201824501004

Sabri, M. M., & Shashkin, K. G. (2018). Improvement of the soil deformation modulus using an expandable polyurethane resin. *Magazine of Civil Engineering, 7,* 222–234. https://doi.org/10.18720/MCE.83.20

Sabri, M. M., Vatin, N. I., & Alsaffar, K. A. M. (2021). Soil injection technology using an expandable polyurethane resin: A Review. *Polymers, 13*(21), Article 3666. https://doi.org/10.3390/polym13213666

Saleh, S., Yunus, N. Z. M., Ahmad, K., & Ali, N. (2019). Improving the strength of weak soil using polyurethane grouts: A Review. *Construction and Building Materials*, *202*, 738–752. https://doi.org/10.1016/j.conbuildmat.2019.01.048

Shi, M., Wang, F., & Luo, J. (2010). Compressive strength of polymer grouting material at different temperatures. *Journal of Wuhan Univiversity of Technology-Mater. Sci. Ed., 25*(6), 962–965. https://doi.org/10.1007/s11595-010-0129-5

Somarathna, H. M. C. C., Raman, S. N., Mohotti, D., Mutalib, A. A., & Badri, K. H. (2018). The use of polyurethane for structural and infrastructural engineering applications: A state-of-the-art review. *Construction and Building Materials, 190*, 995–1014. https://doi.org/10.1016/j.conbuildmat.2018.09.166

Tamošiūnas, T., Žaržojus, G., & Skuodis, Š. (2022). Indirect determination of soil Young's modulus in Lithuania using cone penetration test data. *The Baltic Journal of Road and Bridge Engineering*, *17*(2), 1–24. https://doi.org/10.7250/bjrbe.2022-17.558

Wang, Ch., Guo, Ch., Du, X., Shi, M., Liu, Q., & Xia, Y. (2021). Reinforcement of silty soil with permeable polyurethane by penetration injection. *Construction and Building Materials, 310*, Article 124829. https://doi.org/10.1016/j.conbuildmat.2021.124829

Wei, Y., Wang, F., Gao, X., & Zhong, Y. (2017). Microstructure and fatigue performance of polyurethane grout materials under compression. *Journal of Materials in Civil Engineering*, *29*(9). https://doi.org/10.1061/(ASCE)MT.1943-5533.0001954

Whisler. D., & Kim, H. (2015). Experimental and simulated high strain dynamic loading of polyurethane foam. *Polymer Testing*, *41*, 219–230. https://doi.org/10.1016/j.polymertesting.2014.12.004

Xiang, G., Wei, H., Ya, W., & Yanhui, Z. (2017). Experiment and modelling for compressive strength of polyurethane grout materials. *Acta Materiae Compositae Sinica*, *34*(2*)*, 438–445. https://doi.org/10.13801/j.cnki.fhclxb.20160413.002

Yang, R., Wang, B., Li, M., Zhang. X., & Li, J. (2019). Preparation, characterization and thermal degradation behaviour of rigid polyurethane foam using a malic acid based polyols. *Industrial Crops and Products*, *136*(10), 121–128. https://doi.org/10.1016/j.indcrop.2019.04.073

Zeghal, E., Vaksmaa, A., Vielfaure, H., Boekhout, T., & Niemann, H. (2021). The potential role of marine fungi in plastic degradation – A review. *Journal Frontiers in Marine Science, 8*. https://doi.org/10.3389/fmars.2021.738877

Zhang, Z., Zhong, W., Chen, J., & Luo, J. (2022). Compressive properties and energy absorption of rigid polyurethane foam. *Journal of Physics: Conference Series*, Article 012013. http://doi.org/10.1088/1742-6596/2368/1/012013

Zhong, Y., Xu, Sh., Cao, Ch., Zhang, B., Du, X., Duan, D., Li, X., Hao, M., & Pei, W. (2023). Influence of temperature on the mechanical properties of modified low exothermic polyurethane grouting material and engineering applications. *Journal of Materials in Civil Engineering, 35*(11). https://doi.org/10.1061/JMCEE7.MTENG-15774

Notations

Variables

σ_y – yield stress or peak stress;
σ_z – vertical stress;
z – depth.

Abbreviations

LPF – low-density polyurethane foam;
HPF – high-density polyurethane foam.